Direct Observation of Postadsorption Aggregation of Antifreeze Glycoproteins on Silicates

Ph. Lavalle,[†] A. L. DeVries,[‡] C.-C. C. Cheng,[‡] S. Scheuring,[†] and J. J. Ramsden*[,†]

Biozentrum, University of Basel, Klingelbergstrasse 70, 4056 Basel, Switzerland, and Department of Physiology and Biophysics, University of Illinois, 524 Burrill Hall, 407 S. Goodwin Avenue, Urbana, Illinois 61801

Received December 31, 1999. In Final Form: March 13, 2000

The adsorption of antifreeze glycoproteins (AFGP) from aqueous solution onto two different silicate minerals, muscovite mica and amorphous silica−titania, has been directly observed for the first time in situ using atomic force microscopy (AFM) and optical waveguide lightmode spectroscopy (OWLS). The former yields the lateral distribution and heights of adsorbed single molecules and massed adsorpta, and the latter enables the precise number of adsorbed AFGP per unit area of surface to be determined as well as the kinetics of adsorption and desorption. On both surfaces the AFGP were initially deposited as isolated molecules. On mica they remained as such and could be imaged as compact, globular objects, in contrast to the elongated form presumed to exist in solution. On silica−titania they subsequently formed isolated conical deposits containing large numbers of molecules. The relevance of these results to the adsorption of the AFGP on ice is discussed.

Introduction

Antifreeze glycoproteins (AFGP) are able to effect a remarkable inhibition of ice crystal formation in the blood of some coldwater fishes. Typically, ice-covered waters of the polar seas are near their freezing point of −1.9 °C (in shallow areas, ice is endemic and hence supercooling does not occur). The body fluids of temperate and tropical fish typically freeze between −0.5 and −0.9 °C (and at −0.01 °C after dialysis), essentially due to the familiar colligative freezing point depression. The blood of AFGP-containing Antarctic fishes, however, only freezes at −2.2 °C; i.e., the crucial threshold is crossed.[1]

The serum ingredients responsible for the noncolligative freezing point depression in the Antarctic notothenioid fishes have been identified as antifreeze glycoproteins,[2,3] present at a concentration of about 44 mg/mL serum. They have an unusual amino acid sequence, consisting simply of a repeated triplet (alanine−alanine−threonine).[1] The threonine is glycosylated with a β-D-galactopyranosyl−(1→3)-2-acetamido-2-deoxy-α-D-galactopyranose. Thus the AFGP are quite distinct from colligative antifreeze[4,5] and ice nucleation proteins[6] (cf. circulating lipoproteins in insects[7] and a protein embedded in the cell wall in certain bacteria[8]).

Observations of ice crystal growth under freezing conditions in the presence of antifreeze isolated from coldwater fish serum revealed long needles oriented parallel to the *c* axis.[2] These results have been interpreted by a model[2,3,9] (but see the critique in ref 10) in which the proteins adsorb at isolated positions on the neobasal face of hexagonal ice crystals, blocking further ice formation at those positions and forcing the intervening regions to become more and more highly curved, thereby progressively retarding and ultimately stopping growth. The AFGP is thus a protein with the potential for subtle and selective interactions with different kinds of surfaces. To understand the underlying physicochemical basis for this kind of selectivity, we have embarked on an original program of detailed investigation of the adsorption behavior of the protein at the solid/liquid interface. Previous work on the interfacial interactions has focused on the interface and not on the protein: here we focus on direct observation of the protein.

To characterize the adsorption process as a dynamical event and identify the structures formed, two relatively recent experimental techniques were selected: (i) The first is atomic force microscopy (AFM), in which the surface is scanned by a stylus while monitoring its deflexion as it comes into contact with objects on the surface.[11] By controlling the deflexion via a feedback loop which maintains a constant force between the stylus and the surface, an image of the surface morphology can be constructed.[12] (ii) The second is optical waveguide lightmode spectroscopy (OWLS), in which light is guided parallel to the surface while monitoring its phase velocity.[13] If the velocities of at least two guided modes are measured, the number of adsorbed molecules per unit area can be

* Corresponding author.
[†] University of Basel.
[‡] University of Illinois.

(1) DeVries, A. L. *Comp. Biochem. Physiol.* **1982**, *73A*, 627.
(2) Raymond, J. A.; DeVries, A. L. *Proc. Natl Acad. Sci. U.S.A.* **1977**, *74*, 2589.
(3) Knight, C. A.; DeVries, A. L. *J. Cryst. Growth* **1994**, *143*, 301.
(4) Jia, Z.; DeLuca, C. I.; Chao, H.; Davies, P. L. *Nature (London)* **1996**, *384*, 285.
(5) Davies, P. L.; Sykes, B. D. *Curr. Opin. Struct. Biol.* **1997**, *7*, 828.
(6) Hew, C. L.; Yang, D. S. C. *Eur. J. Biochem.* **1992**, *203*, 33.
(7) Neven, L. C.; Duman, J. G.; Low, J. G.; Sehl, L. C.; Castellion, F. J. *J. Comput. Physiol. B* **1989**, *159*, 71.
(8) Wobler P. K.; Warren, G. J. *Trends Biochem. Sci.* **1989**, *14*, 179.
(9) The crystal plane selectivity of AFGP adsorption was presumed to be a consequence of the distance (9.31 Å, assuming the polypeptide chains to be in the proline helix conformation) between two sugar hydroxyls (i.e. between two threonines) corresponding approximately to twice the distance (2 × 4.52 Å) between hydroxyls on the neobasal face but not to the corresponding distance (7.4 Å) on the basal plane (note however that the 4.52 Å separation is not unique to the prism face). See ref 10 for further discussion and critique, based on a detailed appraisal of antifreeze protein I (AFPI), which shares many structural features with the AFGP.
(10) Harding, M. M.; Ward, L. G.; Haymet, A. D. J. *Eur. J. Biochem.* **1999**, *264*, 653.
(11) Drake, B.; Prater, C. B.; Weisenhorn, A. L.; Gould, S. A.; Albrecht, T. R.; Quate, C. F.; Cannell, D. S.; Hansma, H. G.; Hansma, P. K. *Science* **1989**, *243*, 1586.
(12) Hoh, J. H.; Hansma, P. K. *Trends Cell Biol.* **1992**, *2*, 208.
(13) Ramsden, J. J. *J. Stat. Phys.* **1993**, *73*, 853.

10.1021/la9916934 CCC: $19.00
Published on Web 06/01/2000

Table 1. Attributes of the AFGP

AFGP	M_r/kDa[a]	n[a]	l/nm[b]	l/nm[c]
1	33.7	52	48.4	53.5
2	28.8	44	41.0	45.7
3	21.5	32	29.8	34.1
4	17.0	26	24.2	27.0
5	10.5	16	14.9	16.7

[a] From ref 3. n is the approximate number of disaccharides (equal to the number of amino acid triplets). [b] Assuming the AFGP to have the conformation of a polyproline helix, implying a repeat length of 9.31 Å. [c] Calculated from the OWLS/AFM data as described in the text.

determined with excellent precision. We have combined the two techniques by first measuring the kinetics and absolute amounts of adsorbed protein using OWLS and then transferring the glycoprotein-coated substrates to the AFM for detailed investigation of the morphology.

Experimental Section

Glycoproteins. The AFGP fraction was isolated and separated from the blood serum proteins of the Antarctic notothenioid fish *Dissostichus mawsoni* by ion-exchange chromatography[14] followed by gel filtration on Sephacryl S-100-HR (Sigma) which separated proteins into the various size classes. Experiments were carried out with a mixture of AFGP 1, 2, 3, 4, and 5 (see Table 1), which are present in serum at a concentration of about 4 mg/mL. It was lyophilized and stored at 4 °C and then diluted with water[15] to an appropriate concentration. Sizing column chromatography and ultracentrifugation yielded no evidence for AFGP 1−5 aggregation in water.

Surfaces.[16] For OWLS, a high refractive index material is needed to ensure waveguiding. We used pyrolyzed sol−gel planar waveguides of composition $Si_{0.8}Ti_{0.2}O_2$ equipped with an embossed grating coupler[17] to allow the phase velocities to be conveniently monitored.[18] They were purchased from MicroVacuum, Budapest, Hungary (Type 2400, 12 × 8 mm), and soaked in water[15] for 12 h before use.

For the AFM, both the $Si(Ti)O_2$ waveguides and freshly cleaved muscovite mica glued to a magnetic nickel plate without an intermediate Teflon sheet were used.

Instrumentation. (1) AFM. A Nanoscope III (Digital Instruments, Santa Barbara, CA) was used, equipped with silicon nitride cantilevers having a nominal spring constant of 0.05 N/m and a nominal tip radius of 5−40 nm and a fluid cell to enable the proteins to be imaged in water. The AFM was operated in constant force contact mode (details in ref 19) applying the smallest possible force to avoid perturbing or damaging the sample. Images were recorded with a pixel resolution of 512 × 512 and a scan rate of 2 Hz. They were treated using the Visilog image analysis software (Noesis, Coutaboeuf, France) in order to determine the number and positions of the deposited AFGP 1−5 on the surface. The radial distribution function (pair correlation function) $g(r)$, which describes how adsorbed proteins are organized with respect to each other,[20] was then calculated from these data.

(2) OWLS. A flow-through cuvette was sealed to the waveguide surface. The phase velocities of the guided modes were measured with an IOS-1 integrated optical scanner[21] (Artificial Sensing Instruments, Zürich, Switzerland), modified as described by Kurrat et al.[22] The refractive index increment of the AFGP, needed for calculating the amount of surface-associated protein from the optical data,[23] was measured using an LI3 Rayleigh interferometer (Carl Zeiss, Jena, Germany) and was found equal to 0.142 cm^3/g.

Adsorption Procedures (at Room Temperature). (1) Mica Surfaces. A 100 μL volume of AFGP 1−5 at a concentration of 100 μg/mL was deposited onto freshly cleaved mica and allowed to adsorb for 30 min and then rinsed with 0.2 mL water to avoid contaminating the AFM cantilever and tip with protein from the solution. The proteins were not exposed to air at any time.

(2) $Si(Ti)O_2$ (Waveguide) Surfaces. Adsorption took place while measuring in situ with OWLS: AFGP 1−5 at a concentration of 24 μg/mL constantly flowed through a fluid cell mounted onto the waveguide with a wall shear rate equal to 2.50 s^{-1} until the surface was practically saturated with proteins. Then the glycoprotein solution was replaced with pure water,[15] upon which some desorption occurred, and as soon as a new plateau was reached, the sample was transferred to the AFM, keeping the proteins constantly under water.

Results and Discussion

Figure 1 shows a typical AFM image from a mica deposit. These are the first direct observations of the protein in situ. We identify each feature (whose size ranged between 15 and 30 nm) as an isolated molecule from the glycoprotein mixture. The radial distribution function $g(r)$ shown in Figure 2 was calculated from the images (Figure 1 et al.). The $g(r)$ values are very uniform and close to unity regardless of the distance between the proteins, suggesting a random distribution of adsorbed molecules and no or only very weak interactions between them. The experimental data were compared with the predictions of the random sequential addition (RSA) model, in which hard spheres are deposited onto the surface sequentially at randomly chosen positions and a new particle is irreversibly fixed at the surface only if it does not overlap with any of the previously adsorbed ones (hard body exclusion), otherwise a new trial takes place with a new particle.[24] RSA has been shown to provide an accurate description of the adsorption of globular proteins at the solid/liquid interface.[25] We generated an RSA deposit with same surface coverage as in the protein experiments by simulation and calculated $g(r)$ using the same surface pixelization procedure used to treat the AFM data. The simulated RSA $g(r)$ agrees very closely with the experimental result, supporting the notion that the distribution of the AFGP 1−5 molecules is random without interaction between them other than hard body exclusion. A further inference from the lack of significant structure in the plot of $g(r)$ vs r is that the protein is not preferentially adsorbed at particular atomic positions of the crystalline mica surface.[26]

Figure 3 shows a typical AFM image of a deposit on $Si(Ti)O_2$. The objects differ from those imaged on mica in that (a) they are much larger, both laterally and perpendicular to the surface, and (b) they have a very wide distribution of sizes. More detailed analysis revealed that they are aggregates roughly conical in shape and obeying a definite relation between base diameter and height (Figure 4). While all AFM images of individual objects are to some extent subject to lateral distortion due to the finite radius of the scanning probe tip,[28] the fact that the cones have rather shallow sloping sides implies minimal distortion. The advantage of using the $Si(Ti)O_2$ surface instead

(14) DeVries, A. L.; Komatsu, S. K.; Feeney, R. E. *J. Biol. Chem.* **1970**, *245*, 2901.
(15) All water used was purified in a "Nanopure" installation (Barnstead, OH) and typically had a resistivity of 18 MΩ cm.
(16) Ultimately, investigation of the adsorption on ice using AFM and OWLS is a goal, but this raises presently insuperable technical difficulties.
(17) Lukosz, W.; Tiefenthaler, K. *Opt. Lett.* **1983**, *8*, 537.
(18) Tiefenthaler, K.; Lukosz, W. *J. Opt. Soc. Am. B* **1989**, *6*, 209.
(19) Scheuring, S.; Müller, D. J.; Ringler, P.; Heymann, J. B.; Engel, A. *J. Microsc.* **1999**, *193*, 28.
(20) Wojtaszczyk, P.; Schaaf, P.; Senger, B.; Zembala, M.; Voegel, J.-C. *J. Chem. Phys.* **1993**, *99*, 7198.
(21) Tiefenthaler, K. *Adv. Biosens.* **1992**, *2*, 261.
(22) Kurrat, R.; Textor, M.; Ramsden, J. J.; Böni, P.; Spencer, N. D. *Rev. Sci. Instrum.* **1997**, *68*, 2172.
(23) Ball, V.; Ramsden, J. J. *Biopolymers* **1998**, *46*, 489.
(24) Hinrichsen, E. L.; Feder, J.; Jøssang, T. *J. Stat. Phys.* **1986**, *44*, 793.
(25) Ramsden, J. J. *Phys. Rev. Lett.* **1993**, *71*, 295.
(26) See e.g. ref 27 for the surface structure of mica.
(27) Hunter, R. J. *Foundations of Colloid Science*; Clarendon Press: Oxford, U.K., 1997; Vol. I.

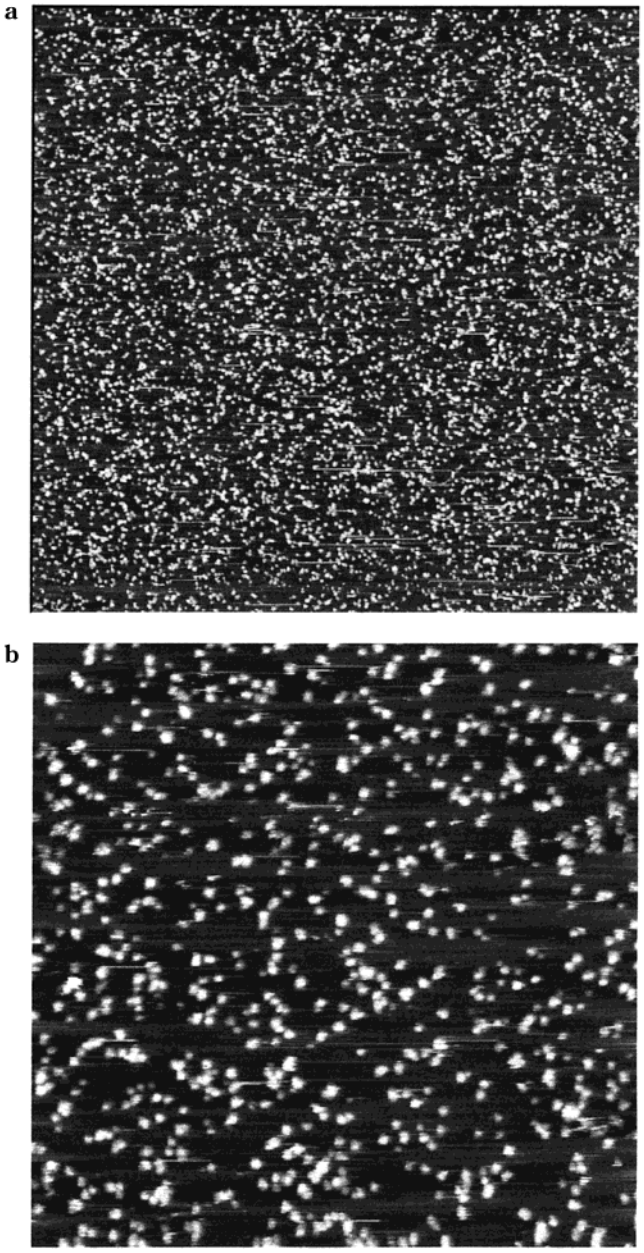

Figure 1. AFM topograph of isolated AFGP 1−5 molecules on mica: (a) image 3 × 3 μm, *z*-scale 3 nm; (b) image is 1 × 1 μm, *z*-scale 3 nm.

of mica is that the exact number of AFGP molecules deposited can be determined by OWLS immediately prior to AFM imaging. Figure 5 shows the glycoprotein adsorption kinetics corresponding to the image of Figure 4. As will be described below, the consecutive determinations of first the total amount of protein associated with the surface and second the shape and size of the aggregates into which they are gathered allows the molecular volume to be determined.

Determination of Molecular Volume. According to the OWLS measurements, 20 ng/cm^2 of glycoprotein remained on the surface after rinsing with water, corresponding to $\nu_1 = 3574$ molecules/μm^2 if all the AFGP are represented by type 1 or $\nu_5 = 11\,471$ molecules/μm^2 if all are represented by type 5.[29] The aggregates have a mean base radius $\bar{r}$ and height $\bar{h}$ of 41.3 and 7.6 nm, respectively, giving a mean cone volume $\bar{v} = \pi\bar{r}^2\bar{h}/3 = 13\,514$ nm^3.

(28) Markiewicz, P.; Goh, M. C. *Langmuir* **1994**, *10*, 5.

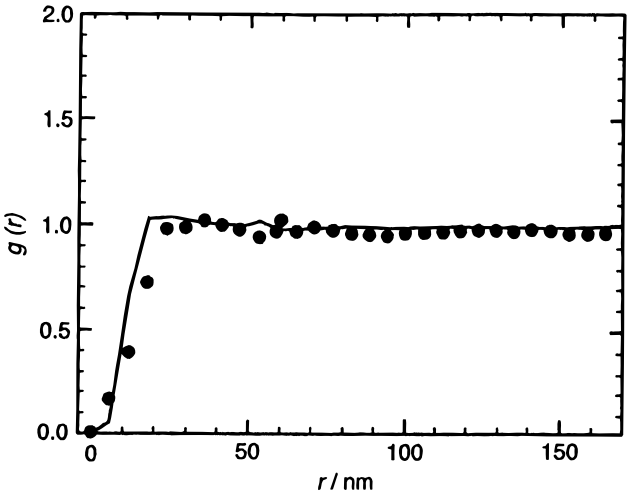

Figure 2. Radial distribution function $g(r)$ as a function of interparticle distances r: black circles, calculated from AFM images of AFGP 1−5 deposited at a surface concentration of 660 proteins/μm^2 on mica (Figure 1); solid line, calculated from a simulated RSA deposit of spheres (radius 5.86 nm) using the same procedure as for the AFM images.

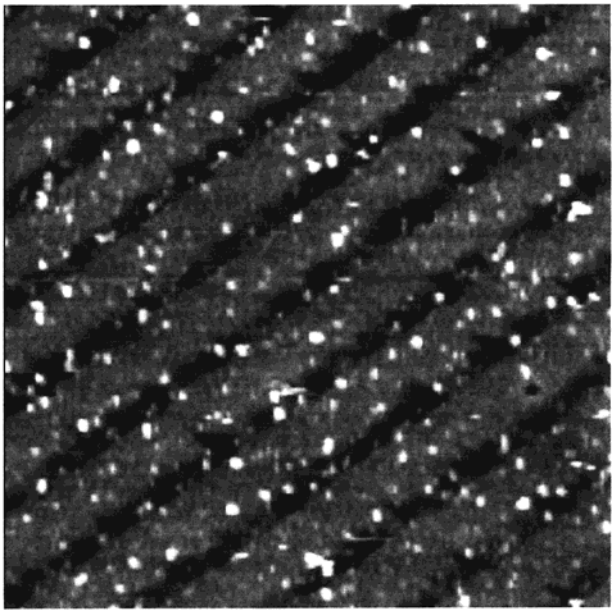

Figure 3. AFM height mode image of AFGP 1−5 on Si(Ti)O_2. The image size is 3 × 3 μm, and the *z*-scale is 20 nm. White spots correspond to AFGP 1−5 aggregates, and black lines to the grating coupler required for the phase velocity detection (grating constant 416 nm, depth 5−10 nm, embossed into the waveguide surface).

Counting all the differently sized aggregates together, there are on average about 25 aggregates per μm^2. We shall call this surface density A. The quotient of ν and A gives the mean numbers of molecules per aggregate—143 and 459 for types 1 and 5, respectively, and finally the volumes v per molecule are given by:[30,31−33]

$$v = \bar{v}/(\nu/A) \qquad (1)$$

giving values of 95 and 29 nm^3 for types 1 and 5, respectively. The protein is assumed to form helical

(29) Since at present we only have available a mixture of the AFGPs whose proportions are not known exactly and which cannot be separated at a reasonable yield, we start with calculations assuming either of the two extreme situations: either all the proteins are AFGP 1 (the largest) or all are AFGP 5 (the smallest).

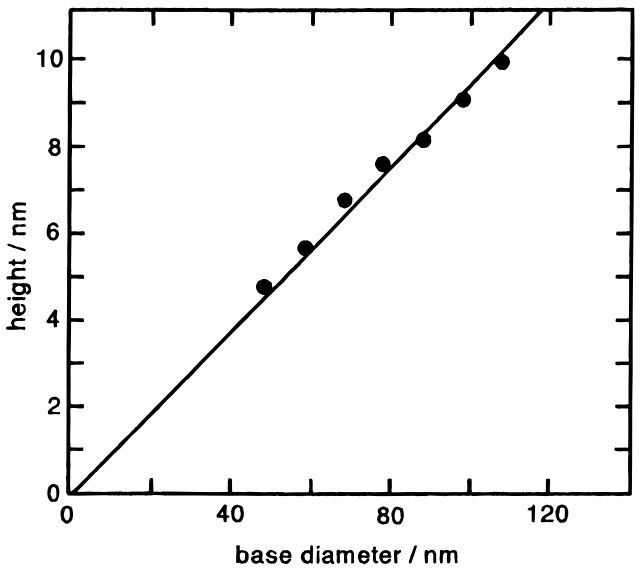

Figure 4. Relationship between base diameter and height for 360 conical aggregates. (See Figure 5 for their adsorption history.) Filled circles correspond to mean heights from experimental measurements after regrouping base diameters into bins. The slope of the solid line is 0.093.

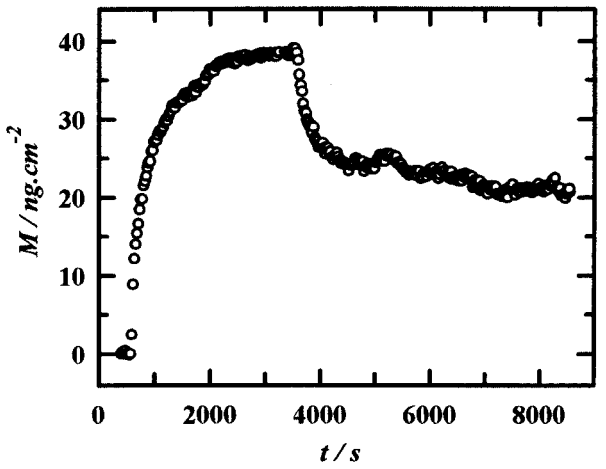

Figure 5. Typical plot of the association of a mixture of AFGP 1−5 dissolved in water and flowing over a $Si(Ti)O_2$ surface. Bulk concentration = 24 μg/mL, and wall shear rate = 2.50 s^{-1}. Flow began at t = 687 s, and the glycoprotein solution was replaced by pure water at t = 3624 s.

polyproline cylinders.[3,34] We estimate their diameter d from molecular models as 1.5 nm, which yields lengths $l = v/(\pi(d/2)^2)$ of 53.5 and 16.7 nm for types 1 and 5, respectively, in good agreement[35] with estimates[3] based on a repeat length of 0.931 nm when the protein is in the polyproline helix conformation.[1]

The above estimates do not in themselves yield information on the shape of the AFGP. The images of isolated individual molecules on mica show that the protein molecules have a compact, nonelongated structure, rather than that of an extended cylinder. Since structural studies of the protein in solution using light scattering, viscosity, NMR, etc., indicate an extended structure,[13,36,37,38] it must be inferred that the protein undergoes a considerable conformational change upon adsorption.

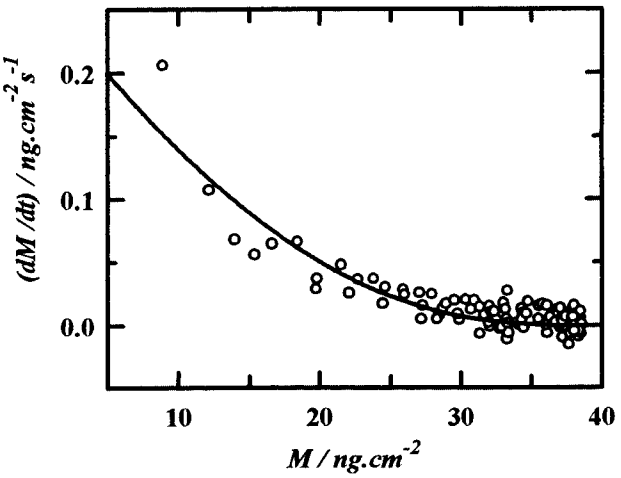

Figure 6. Data of Figure 5 numerically differentiated and plotted (circles) as the rate of adsorption versus amount adsorbed. The solid line shows the RSA polynomial (eq 31 in ref 41; note that when desorption takes place, the third-order coefficient slightly increases,[38] but this is such a small effect that it was neglected in the fitting) fitted to the data with a ($=\theta/\nu$, where θ is the fractional surface coverage) as the free parameter.

Kinetic Analysis. The adsorption kinetics (Figure 5) follow the predictions of RSA.[35] This can be seen most easily by plotting dM/dt vs M for the adsorption phase of the experiment (Figure 6); the data lie on a characteristically concave curve, which was observed for all experiments. If the proteins were laterally mobile and formed two-dimensional clusters or crystals following initial adsorption, the plot of dM/dt vs M would be linear with negative slope,[39] and were the AFGP arriving at the surface practically only able to adhere at aggregates already existing, then the rate of adsorption dM/dt would be constant up to the point where the aggregates themselves started interfering with each other.[40] Since neither of these types of behavior were observed, we must conclude that the initial event is monomers adsorbing randomly and sequentially.

The theoretical RSA kinetics[41] were fitted to the data with a free parameter a, the mean area per molecule at the moment of adsorption. We found a = 51 nm^2. Since for a cylindrical monomer $a = ld$, this value is well within the range expected (the mean length (Table 1) multiplied by d = 1.5 nm gives a = 47.5 nm^2).

Since the amount of AFGP adsorbed as the binding nears saturation (see Figure 5; it is about 38 ng/cm^2) is that expected for RSA at the jamming limit (i.e. a fractional coverage of 0.55 for disks [24] or spherocylinders of an aspect ratio of 1:4 [42]), it would appear that the aggregation into cones occurs subsequently.[43] From the observation (Figure 5) that 44% of the deposited material is removed

(30) See refs 31−33 for recent discussion of some of the problems associated with protein volume determination using atomic force microscopy.

(31) Fritzsche, W.; Henderson, E. *Scan. Microsc.* **1996**, *10*, 103.

(32) Schneider, S. W.; Larmer, J.; Henderson, R. M.; Oberleithner, H. *Pfluegers Arch.* **1998**, *435*, 362.

(33) Scheuring, S.; Ringler, P.; Borgnia, M.; Stahlberg, H.; Müller, D. J.; Agre, P.; Engel, A. *EMBO J.* **1999**, *18*, 4981.

(34) Knight, C. A.; Driggers, E.; DeVries, A. L. *Biophys. J.* **1993**, *64*, 252.

(35) The overestimation (~10%) may be due to the disaccharides, whose contribution has not been taken into account in estimating the diameter.

(36) Rao, B. N. N.; Bush, C. A. *Biopolymers* **1987**, *26*, 1227.

(37) Wilson, P.; DeVries, A. L. *Cryo-Lett.* **1994**, *15*, 127.

(38) Tarjus, G.; Schaaf, P.; Talbot, J. *J. Chem. Phys.* **1990**, *93*, 8352.

(39) Ramsden, J. J.; Bachmanova, G. I.; Archakov, A. I. *Phys. Rev. E* **1994**, *50*, 5072.

(40) Ball, V.; Ramsden, J. J. *J. Phys. Chem. B* **1997**, *101*, 5465.

(41) Schaaf, P.; Talbot, J. *J. Chem. Phys.* **1989**, *93*, 4401.

(42) Viot, P.; Tarjus, G.; Ricci, S. M.; Talbot, J. *J. Chem. Phys.* **1992**, *97*, 5212.

upon dilution (rinsing), one may infer either that aggregation competes with desorption and the aggregates do not desorb or that dilution selects AFGPs adsorbed in a weakly binding orientation or conformation, and once they have been removed those remaining have space to migrate laterally and condense in the conical aggregates seen on the AFM images. The latter explanation seems more likely, since, in the former, some aggregates should be able to form before the coverage becomes crowded enough to hinder lateral migration, whereas the actual value of the saturation limit is consistent with a jammed randomly sequentially adsorbed monolayer.

Conclusions

(1) AFGP 1−5 dissolved in pure water adsorb according to the mechanism of random sequential addition, as evinced by either the adsorption kinetics and jamming limit or the radial distribution function, onto hydrated $Si(Ti)O_2$ or muscovite mica surfaces.

(2) Rinsing with pure water after adsorption results in rapid desorption of about half of the adsorbed material.

(3) AFGP adsorbed on mica are present as isolated molecules in a compact, globular conformation. If they indeed exist as elongated polyproline helices in solution, it thus seems that they undergo a conformational change upon adsorption (i.e. a kind of epitaxy).

(4) AFGP adsorbed on $Si(Ti)O_2$ and imaged after rinsing is massed into conical aggregates of a definite shape but varying sizes, containing hundreds of molecules. Since the initial process of adsorption (1, above) implies the adsorption of individual isolated molecules, aggregation must be a postadsorption process, requiring the glycoproteins to be mobile on the surface. Once aggregated, the AFGP appears to be desorption resistant, but as monomers, the proteins may be present at the surface in both a low affinity and a high affinity form.

(5) The contrasting behavior of the proteins on $Si(Ti)O_2$ and muscovite mica can be most easily interpreted by supposing that the proteins are not mobile on mica. While both materials are silicates (e.g. ref 27), they also show significant differences in the arrangement and type of other atoms which make up their structures,[26] resulting in different decay profiles perpendicular to the adsorbing surface of the major forces involved in protein−surface interaction.[44] The present results hint at a correlation between these profiles and the adsorption behavior, which probably goes beyond the energetics of adsorption of individual molecules. Since it is unlikely that the spatial arrangement of the hydroxyl groups of either muscovite mica or silica−titania match those of the neobasal face of ice, the very fact that we observe significant adsorption on these materials (albeit in the presence of water!) argues against a crucial role of hydroxyl matching in the antifreeze action of the protein and lends support for the notion that the origin of the still mysterious ice crystal plane specificity of the antifreeze action of the AFGP is due to such profiles,[45] rather than the fortuitous matching of certain chemical groups.

Acknowledgment. The authors wish to express their gratitude to the Freie Akademische Gesellschaft, Basel, for financial support and INSERM U424 (Strasbourg, France) for image analysis facilities.

LA9916934

(43) Using the relation $a = M_r\theta_J/(N_A M_{sat})$, where M_r is molecular mass and N_A Avogadro's number and the jamming coverage $\theta_J = 0.547$, we calculate for the two extremes $a = 77$ and $a = 24$ nm^2 for all AFGP 1 and all AFGP 5, respectively.

(44) Cacace, M. G.; Landau, E. M.; Ramsden, J. J. *Q. Rev. Biophys.* **1997**, *30*, 241.

(45) Haymet, A. D. J. *Proceedings of the International CECAM Workshop on Molecular Modelling of Proteins at Interfaces*; CECAM: Lyon, France, Sept 1999.